

Characteristics of 23 MV Photon Beam from a Mevatron KD 8067 Dual Energy Linear Accelerator

Ok Bae Kim, M.D., Tae Jin Choi, M.S. and Young Hoon Kim, M.D.

Department of Therapeutic Radiology, School of Medicine, Keimyung University, Taegu, Korea

The characteristics of 23 MV photon beam have been presented with respect to clinical parameters of central axis depth dose, tissue-maximum ratios, scatter-maximum ratios, surface dose and scatter correction factors.

The nominal accelerating potential was found to be 18.5 ± 0.5 MV on the central axis.

The half-value layer (HVL) of this photon beam was measured with narrow beam geometry from central axis, and it has been showed the thickness of 24.5 g/cm^2 .

The tissue-maximum ratio values have been determined from measured percentage depth dose data.

In our experimental dosimetry, the surface dose of maximum showed only 9.6% of maximum dose at $10 \times 10 \text{ cm}^2$, 100 cm SSD, without blocking tray in. The TMR'S of 0×0 field size have been determined to get average 2.3% uncertainties from three different methods; are zero effective attenuation coefficient, non-linear least square fit of TMR's data and effective linear attenuation coefficient from the HVL of 23 MV photon beams of dual energy linear accelerator.

Key Words: 23 MV photon beam, TMR, SMR, Surface dose

INTRODUCTION

The characteristics of the megavoltage photon beam from linear accelerators depend not only on the nominal energy of the electrons in the waveguide at the exit window, but on the energy spread in the basms, flattening filter, ion chamber and collimating systems.

Recently, Donald A. Johnson¹⁾ and JM Paul et al²⁾ have characterized the parameters of 18 MV photon beam with Clinac 1800 and 15 MV with Mevatron 77, respectively. But the properties of the 23 MV photon beams were not characterized at any published papers.

We have evaluated with dosimetric characteristics of the 23 MV photon beams of Mevatron KD 8067.

In high energy X-ray beams, even of the same nominal energy may have different dosimetric characteristics due to differences in target and collimating system.

It is the purpose of this paper to present the clinical dosimetry data so that the user or potential user of a high energy accelerator may compare to the characteristics of this 23 MV photon beams with

the user's own measured data or with the already published characteristics of the other high energy photon beams.

MATERIALS AND METHODS

We have used the following systems for determining the various beam characteristics; 1) WP-600 three dimensional scanner (Wellöfer, Germany) with 0.14 ml dual ion chambers which one of them is for scan and the other is for reference chamber. 2) Parallel-Plate ion chamber Capintec model PS-033 fitted in the center of a polystyrene solid phantom ($\rho = 1.04 \text{ g/cm}^3$) to provide a flat 25×25 square fields.

In the measurements of buildup and surface doses, the thin window of parallel-plate chamber was perpendicular to and facing to the direction of the central ray of the beam, and in the same as the front surface of the polystyrene phantom at distance of 100 cm.

The effective point of measurement for the parallel-plate chamber was taken to be the front surface of the proximal electrode. Doses in the buildup region were measured in the polystyrene phantom with the parallel-plate chamber and were corrected to zero chamber volume using the method described by Velkely et al³⁾.

The percent depth doses at SSD 100 cm were

This study was partly supported by 1989 Research grant from the Keimyung University foundationship.

determined on the central axis of beam in water phantom. The percent depth doses, beam flatness and symmetry profiles at various depths were obtained with 0.14 ml ion chambers Model IC-10 of which wall is air equivalent materials and water proof in the WP-600 water phantom. The positioned accuracy and reproducibility of all three axis on the water phantom was 1.0 mm over 30 cm depth. A reference chamber without buildup cap positioned at a fixed point in the beam was used with WP-600 water phatom system to correct for accelerator output variations during all ion collections.

Tissue maximum ratios (TMR's) were derivered from percentage depth doses data. The TMR's were also measured on the field sizes of 5×5, 10×10, 20×20 and 30×30 cm² at depths of 5, 10 and 20 cm.

The temperature and pressure were monitored

for correction of TMR's measurements and output monitor where changes occured during the data aquisition.

In the measurement of output factor and phantom scatter factor for small fields, the ionization chamber was set as 200 and 300 cm distances for small opening collimator to sufficiently covere the mini-water phantom (7×7×7 cm³ of plastics water phantom)^{1,4)}.

The half value layer and effective linear attenuation coefficient of this photon beam was measured with narrow beam geometry.

RESULTS

1. Central Axis Percent Depth Dose

Percent depth doses were measured for field size from 4×4 cm² to 36×36 cm² at 100 cm source-

Table 1. Percentage Depth Dose of 23 MV Photon Beam, Mevatron KD 8067 Dual Energy Linear Accelerator, SSD = 100cm. (Percentage depth dose values scaled by a factor 10)

Depth (cm)	Field size (cm ²)											
	0x0	4x4	6x6	8x8	10x10	12x12	16x16	20x20	24x24	28x28	32x32	36x36
3.0	990	990	988	989	991	997	998	999	999	1000	1000	1000
3.2	995	994	994	995	996	999	999	999	1000	999	999	999
3.3	997	998	998	998	999	999	1000	1000	999	999	999	999
3.4	998	998	998	999	999	1000	1000	998	998	997	997	996
3.5	999	999	999	1000	1000	999	999	998	998	997	996	996
3.7	1000	1000	1000	999	999	998	997	994	994	993	993	993
3.8	1000	1000	999	998	998	997	997	993	992	991	990	990
4.0	997	997	997	997	996	995	994	988	988	987	986	985
5.0	964	978	977	977	975	971	967	961	960	958	958	958
6.0	926	944	945	943	941	939	935	930	928	928	926	925
7.0	880	906	911	909	909	903	901	898	896	896	896	895
8.0	842	870	870	869	869	874	868	866	866	866	866	864
9.0	809	835	832	835	835	834	835	835	835	837	835	834
10.0	769	804	803	802	802	802	803	805	800	803	803	804
12.0	704	735	736	741	740	743	745	746	747	749	750	750
14.0	643	667	670	683	689	690	690	689	692	698	699	701
15.0	614	638	642	650	659	664	667	670	670	668	674	676
18.0	539	558	570	577	582	587	593	594	599	601	605	602
20.0	493	513	522	529	539	542	548	553	555	561	560	561
22.0	451	471	480	487	494	501	506	514	514	517	520	524
24.0	413	431	440	450	459	464	470	475	479	483	484	485
26.0	378	396	404	416	421	428	436	441	441	447	447	451
28.0	343	364	374	381	389	393	402	409	412	416	418	419
30.0	308	334	343	352	358	365	373	378	382	384	388	389

skin distance (SSD).

These data are presented in Table 1. The percentage depth dose data were normalized to dose of the maximum on the central axis (d_{max}) for each field size.

D_{max} were taken to be the peak of the depth ionization curve. It was found to decrease from 3.8 cm for a 4×4 cm² field size to 2.8 cm for a 36×36 cm² field size. The depth of maximum dose decreased by 1.0 cm as the field size was increased as shown in Table 2.

Since d_{max} decreases as the field size increase, this method of normalization naturally results in decrease of percentage depth doses with increasing field size for shallow depths^{1,5)}

At greater depth, however, the percentage depth doses exhibit the more typical behavior of increase with increasing field sizes. The observed percentage depth dose for a 10×10 cm² field with

100 cm SSD at a depth of 10 cm is $80.2 \pm 0.1\%$, and the depth of 80% dose is 10.1 ± 0.1 cm.

The ratio of the percentage depth dose of large field size (36×36 cm²) to that of small field (4×4 cm²) shows that is small changed within 2% in shallow depth but it shows 9.4% of difference in 20 cm depth.

The depth dose curves for 4×4 cm², 10×10 cm² and 20×20 cm² field sizes are compared in Fig. 1.

2. Flatness and Symmetry

For selected field size, the largest (A) and smallest (B) measured values were taken within the central 80% of the field constitute the region of evaluation from dose distributions plotted for cross and inplane at the depth of 10 cm. The flatness was determined from following relation:

$$\text{Flatness (\%)} = (A - B) \times 100 / (A + B)$$

The measured 23 MV photon beam profiles

Table 2. Variations of Dmax Depth of 23 MV X-rays of Mevatron KD 8067 Dual Energy Linear Accelerator

Field size (cm ²)	4x4	6x6	8x8	10x10	15x15	20x20	24x24	28x28	32x32	36x36
Dmax depth (cm)	3.8	3.7	3.6	3.5	3.4	3.3	3.2	3.0	2.9	2.8

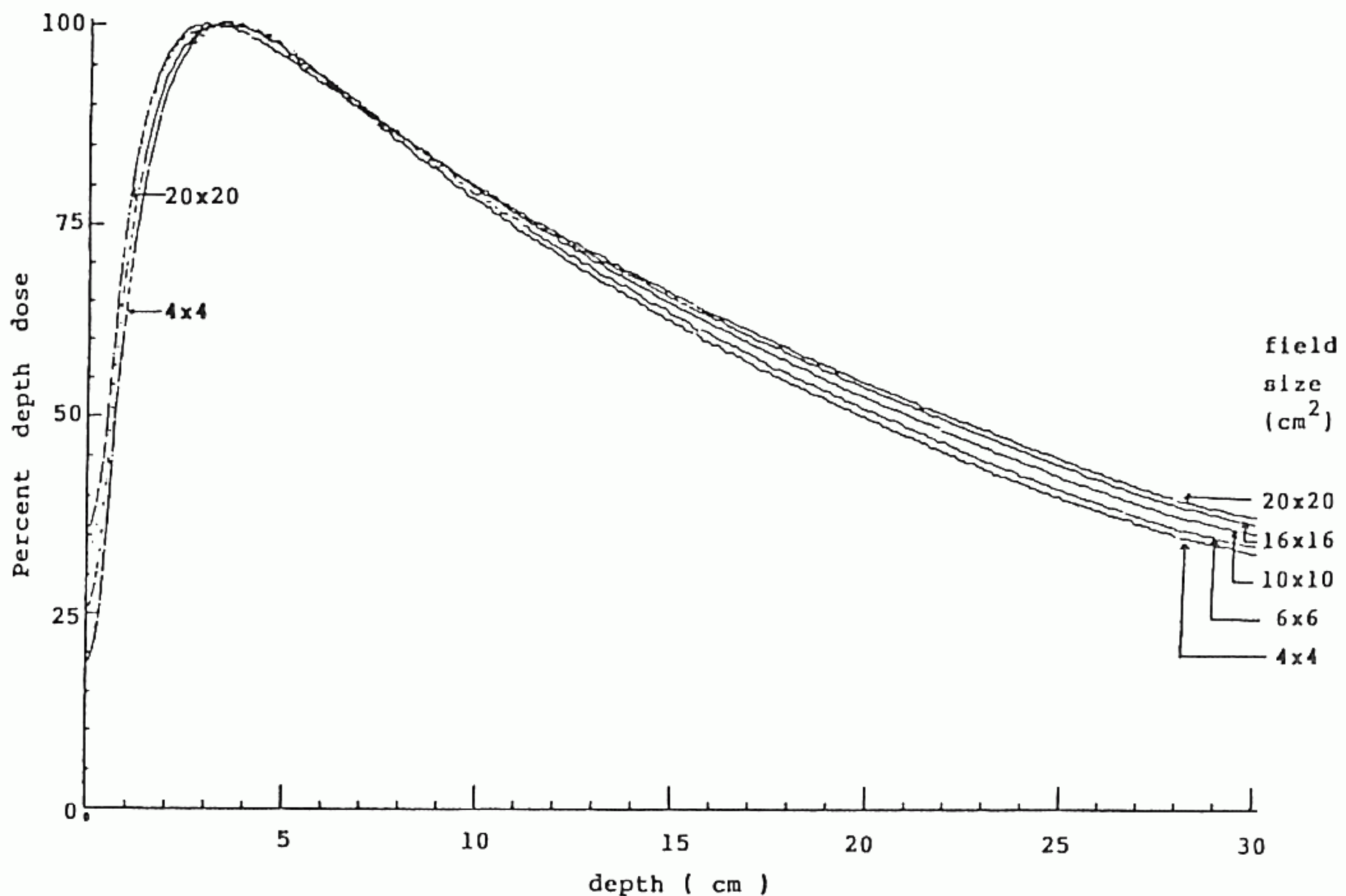


Fig. 1. Central axis depth dose curves for different field sizes at 100 cm SSD for 23 MV X-rays, Mevatron KD 8067.

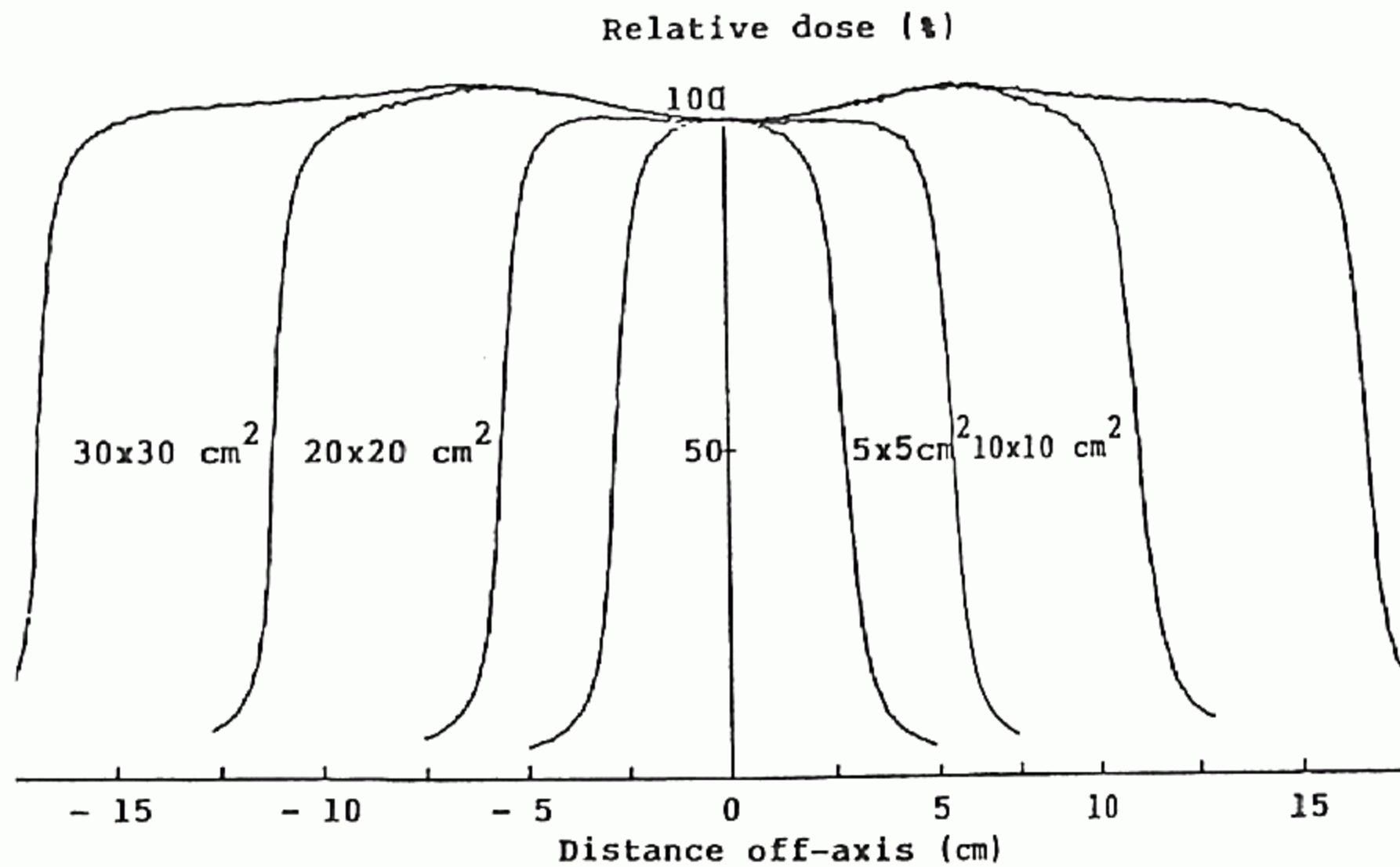


Fig. 2. Relative dose profiles of transverse axis at 10 cm depth for square fields with 5×5, 10×10, 20×20, and 30×30 cm² at distance of 100 cm SSD, 23 MV photon beam of Mevatron KD 8067.

showed the flatness specifications of $2.7 \pm 1.48\%$ of the average values.

The X-ray field symmetry is determined from the dose integrals of the opposite fields halves. Dose integrals were obtained through the tracing of plotted dose profiles of the depth of 10 cm by using the digitizer of personal computer. And the symmetry was determined from following relation;

$$\text{Symmetry (\%)} = |S_1 - S_2| \times 200 / (S_1 + S_2)$$

where S_1 and S_2 are integral areas of each half profile.

In our experiments, the symmetry specifications of $1.13 \pm 0.79\%$ variation in integrated dose over opposited field halves within the dose variation across the central 80% of the beam as shown in Fig. 2 and Table 3.

The dose variation across the central axis at a depth 10 cm for square fields with sides of 5, 10, 20 and 30 cm² are shown in Fig. 2, and the dose was normalized to 100% on central axis at 10 cm depth.

The most common method of specifying the complete absorbed dose distribution within a single radiation beam is by means of the isodose chart. The isodose curves were generated by the RTP computer with profiles of depth dose for the 10×10, and the 30×30 cm² field sizes are compared the one-half of 10×10 and 30×30 cm² fields at 100 cm SSD in Fig. 3. The isodose curves have been showed the small difference of depth dose at shallow depth, but the large off-axis doses.

Table 3. Variations of Beam Flatness and Symmetry of 23 MV X-rays of Mevatron KD 8067 Dual Energy Linear Accelerator in 10cm Depth of Water

Field size (cm ²)	5x5	10x10	20x20	30x30
Flatness (%)	4.9	1.6	2.1	2.3
Symmetry (%)	0.9	2.1	1.3	0.2

3. Buildup and Surface Dose

Measurements of determine the depth dose in buildup region and surface dose were made in a polystyrene phantom using a Capintec Model PS-033 parallel-plate ionization chamber having a 0.0036 mm thin aluminized-polyester film, a volume of 0.5 ml, a diameter of 16 mm and a plate spacing of 2.4 mm.

The chamber could be fitted into a 25×25 cm² polystyrene phantom, with the upper chamber electrode lying in plane of the phantom surface. The density of the polystyrene used was determined to be 1.04 g/cm³ ⁶⁾.

The measurements of depth dose in the buildup region were performed at 100 cm SSD, and the data were normalized to the maximum ionization for the respective field sizes.

Furthermore, in measurement of surface dose, all ionization measurements were corrected to zero

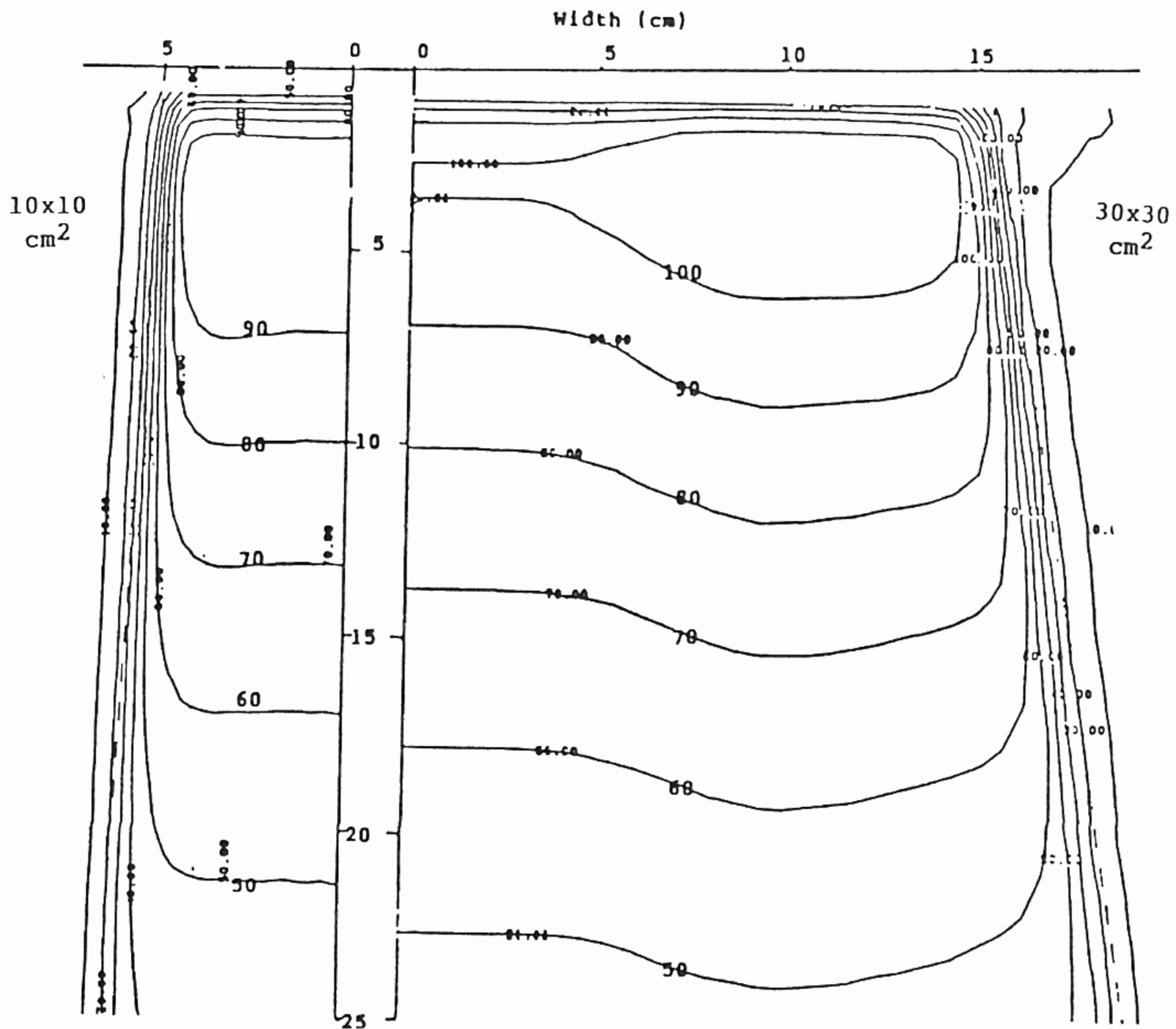


Fig. 3. The isodose curves for one-half of 10×10 and 30×30 cm² field sizes at 100 cm SSD, 23 MV photon beams of Mevatron KD 8067.

chamber volume using the method described by Velkely et al. The corrected percentage (P') of maximum ionization is given by

$$P'(d) = P(d) - \xi(E, d/d_{max}) \times l$$

where l is the plate separation in mm, d is the depth to front surface of chamber, d_{max} is depth of maximum buildup, E is the nominal maximum energy of photon spectrum and ξ is chamber thickness correction factor.

Percentage surface dose data were smoothed with non-linear least square fit and it has less than 0.2% uncertainties to compare with calculated and measured data.

The percent surface doses showed the 9.6%, 21.4% and 25.4% for 10×10 , 20×20 and 25×25 cm² field sizes without blocking tray in, respectively.

The relative percent depth doses in the buildup region and surface dose vs. field sizes are shown in Table 4.

4. TMR and SMR

The depth of the peak dose for the photon beam in water was found to be from 3.8 g/cm² for 4×4 cm² to 2.8 g/cm² for 36×36 cm² field sizes at SSD 100 cm. The ionization charge at depth of maximum was used to normalize the data for determining tissue-maximum ratio (TMR).

TMR's were also calculated from the percentage depth dose using the conversion equation described in Ref. 5, and calculated TMR data are shown in Table 5.

$$\text{TMR}[d,s] = 0.01 \times P[d,f,s'] \frac{S_p[s']}{S_p[s'']} \left(\frac{f+d}{f+d_m} \right)^2$$

where P is percentage depth dose, f is SSD, s' is the $s \cdot f / (f+d)$, s'' is the $s \cdot f / (f+d_m)$ and S_p is the phantom-scatter factor.

The percent difference between the calculated and measured TMR's for selected field sizes and

Table 4. Field Size Dependence of % Surface dose for 23MV Photon Beam, Mevatron KD 8067, with and Without Blocking Tray Thickness of 0.6cm Plastics

Field size [cm ²] depth [mm]	5x5 tray		10x10 tray		20x20 tray		25x25 tray	
	out	in	out	in	out	in	out	in
0.0	3.3	4.2	9.6	10.7	21.4	24.7	25.4	31.1
1.0	15.6	16.0	21.7	22.8	33.4	36.8	37.2	43.0
2.0	24.2	24.6	30.1	31.2	41.4	44.6	44.8	50.4
3.0	32.2	32.5	37.8	38.9	48.6	51.7	51.8	57.2
5.0	46.1	46.4	51.4	52.4	61.3	64.1	64.0	68.9
10.0	71.6	71.9	75.6	76.5	83.1	85.2	84.8	88.4
15.0	85.9	86.4	88.6	89.6	93.9	95.2	95.0	97.1
20.0	92.7	93.4	94.1	95.1	97.5	98.0	98.1	98.9
25.0	95.2	96.0	95.7	96.6	97.5	98.2	99.1	99.3
30.0	99.0	97.5	99.1	99.2	99.9	99.9	100.0	100.0
35.0	100.0	100.0	100.0	100.0	99.9	99.8	99.3	99.3

Table 5. Tissue—Maximum Ratios of 23 MV X-rays, Mevatron KD 8067, SAD=100cm. (TMR values scaled by a factor 1000)

Depth (cm)	Field size (cm ²)											
	0x0	4x4	6x6	8x8	10x10	12x12	16x16	20x20	24x24	28x28	32x32	36x36
3.0	964	974	975	979	981	988	990	993	995	998	998	1000
3.5	987	993	995	1000	1000	1001	1001	1002	1004	1005	1004	1006
3.7	993	998	1000	1003	1003	1004	1003	1002	1004	1005	1005	1007
4.0	1000	1003	1003	1007	1006	1007	1006	1003	1004	1005	1004	1005
5.0	994	999	1002	1005	1004	1002	998	993	993	994	993	995
6.0	971	978	987	990	988	987	984	980	979	980	980	980
7.0	948	959	969	972	972	969	965	964	963	964	964	966
8.0	924	935	944	947	945	950	948	945	946	949	949	951
9.0	907	914	920	925	925	926	926	928	930	934	934	934
10.0	869	884	904	907	905	907	908	910	910	910	913	915
12.0	824	842	858	865	866	868	871	874	877	880	882	885
14.0	764	799	809	820	830	837	837	837	839	845	851	854
15.0	741	774	787	797	806	815	821	825	829	831	829	836
18.0	683	716	730	744	750	757	765	771	773	781	784	788
20.0	638	675	692	704	712	724	731	737	744	748	755	759
22.0	610	641	657	669	676	685	697	704	714	716	719	723
25.0	558	595	606	618	630	639	651	659	664	670	675	682
28.0	520	549	559	572	580	590	601	612	621	628	633	638
30.0	482	515	529	541	552	560	575	585	592	599	604	607

depths are shown in Table 6. The average relative percent difference in the calculated and measured TMR's data showed within $0.3 \pm 0.5\%$ for all select-

ed field and $0.4 \pm 0.4\%$, $0.1 \pm 0.3\%$, $0.1 \pm 0.5\%$ and $0.7 \pm 0.5\%$ for field sizes 5×5 , 10×10 , 20×20 and 30×30 cm², respectively.

The zero area for TMR value was determined by three different methods. In the first method, the TMR data as a function of field size were extrapolated to zero field size by use the polynomial regress. And calculated TMR's were within 0.1% uncertainty to original TMR's for selected square fields. The zero area for TMR's are also shown in Table 5.

In the second method, the zero area effective attenuation coefficient was determined by using the effective attenuation coefficient.

The exponential portion of the TMR curve for each field size was used to calculate an effective attenuation coefficient (μ) using the relation:

$$\mu = 1/10 \ln (\text{TMR}_{20/10})$$

where $\text{TMR}_{20/10}$ is the ratio of the TMR's at depth of 20 cm to that of 10 cm depth. A linear-quadratic least-squares fit to the attenuation coefficient as a

function of field size was used to compute a zero area attenuation coefficient of $0.0283 \text{ cm}^{-1} \pm 0.0002$.

In the third method, the attenuation coefficient was determined from the measurement of half-value layer (HVL) with narrow beam geometry. The thickness of HVL showed 24.5 g/cm^2 and the calculated μ was 0.0283 cm^{-1} . The effective attenuation coefficient was compared to two different method within 0.0001 unit of coefficient.

In the comparison of original calculated TMR from percentage depth dose and obtained TMR by using the least-square fit to polynomial, they are differed by average of ± 0.003 units of percent per point with a maximum variation of less than 1%.

The zero area TMR's estimated by these three methods agree within 2.3% for depths of 5 to 30 cm.

The scatter-maximum ratios (SMR's) were calculated from the square field of TMR's and equation;

$$\text{SMR}(d,f) = \text{TMR}(d,r) S_p(r_d)/S_p(0) - \text{TMR}(d,0)$$

where $S_p(r_d)$ is the phantom scatter correction factor for a given field at depth d , and $S_p(0)$ is the ratio of BSF for a given field radius r to that of for the reference field ($10 \times 10 \text{ cm}^2$)⁷⁾.

These SMR's data are very useful in calculating the dosage to points in tissue from irregularly shaped fields, and the data are shown in Table 7.

Table 6. Percentage Differences in Measured and Calculated Tissue—Maximum Ratios of 23MV Photon Beam, Mevatron KD 8067

depth (cm)	Field size (cm^2)			
	5x5	10x10	20x20	30x30
5.0	0.1%	0.0%	0.0%	0.1%
10.0	0.8%	0.2%	1.1%	1.2%
20.0	0.4%	-0.4%	-0.2%	0.7%

Table 7. SMR Data for 23 MV Photon Beam, Mevatron KD 8067. (SMR values scaled by a factor 1000)

Depth [cm]	Radius [cm]										
	1	2	3	5	8	10	15	20	25	30	50
3.0	6	11	14	21	27	29	33	34	35	35	35
3.5	3	6	8	11	14	16	18	19	19	19	19
4.0	1	2	2	3	4	4	5	5	5	5	5
5.0	1	1	1	2	2	3	3	3	3	3	3
6.0	2	3	4	6	8	8	9	10	10	10	10
7.0	3	5	7	10	13	14	16	17	17	17	17
8.0	5	8	12	17	21	23	26	27	28	28	28
9.0	5	9	12	17	22	24	27	28	29	29	29
10.0	8	14	20	28	36	40	45	47	47	48	48
12.0	10	18	24	35	45	49	55	57	58	59	59
15.0	15	28	38	55	70	77	87	90	92	93	93
18.0	17	32	43	62	80	87	98	102	104	105	105
20.0	20	37	50	72	92	101	114	119	121	121	121
22.0	18	34	47	67	86	95	106	111	113	113	113
25.0	16	30	42	63	83	95	112	120	124	127	129
30.0	17	31	44	65	88	99	116	125	129	132	134

Table 8. Output Factors of 23 MV X-rays, Mevatron KD 8067 (Scaled by a factor 1000)

Field size [A/P]	0	1.0	1.5	2.0	2.5	3.0	4.0	5.0	6.0	7.0	8.0	8.75
Sc	871	935	964	980	1000	1010	1028	1037	1040	1041	1043	1046
Sp	990	993	995	998	1000	1003	1010	1016	1023	1028	1031	1033

In Table 7, calculated SMR data have been smoothed and extended to large field by achieved fitting the SMR's of given field size to the equation

$$\text{SMR}(d,r) = \beta_d (1 - e^{-\alpha_d r})$$

where β_d and α_d are constants⁸⁾.

In our study of the SMR'S, they have been evaluated the average $3.3 \pm 2.0\%$ uncertainties at the large depths.

5. Attenuation Coefficient

The HVL of polystyrene filter was measured from the central axis of the beam, using a narrow-beam geometry.

For small field as $4 \times 4 \text{ cm}^2$, the equilibrium mass is not sufficiently irradiated at the 100 cm distance. Hence, the measurement was performed at distance of 200 cm from the source to mini-water phantom, and the field size was showed $8 \times 8 \text{ cm}^2$ at the phantom surface. The polystyrene blocks for attenuator were mounted between the source and ionization chamber at distance of 100 cm from the source. Especially, this ionization chamber was set at the distance of 200 cm from the building-wall to minimize the effect of backscatter rays⁹⁾.

Calculated the attenuation coefficient from measured data was 0.0283 cm^{-1} , and the half value layer was calculated with 24.5 g/cm^2 . And this value is very close to the zero area effective attenuation coefficient.

6. Relative Output Factors

The relative output factor (ROF) is defined as the ratio of the dose output for a given field to that of a reference field $10 \times 10 \text{ cm}^2$ at 100 cm SSD. The ROF is applied here to determine the output at the depth of dose maximum as a function of the field size.

Table 8 shows the collimator scatter correction (S_c) factors which is commonly called output factor and phantom scatter correction factor which is related to the changes in the area of the phantom irradiated for a fixed collimator opening. As shown by Khan et al¹⁰⁾, the assessment of these factor is very important to calculate the dose distributions.

The dose rate in free space was measured at the

100 cm Source phantom surface distance with mini-water phantom ($7 \times 7 \times 7 \text{ cm}^3$ volume with thickness of 1 mm plastics) for making the electron equilibriums in 23 MV photon beams.

For fields smaller than $7 \times 7 \text{ cm}^2$, the equilibrium mass is not sufficiently supplied at the 100 cm SSD. Hence, the measurements were repeated for $10 \times 10 \text{ cm}^2$ and all small fields at the distances of 200 and 300 cm from the source. Especially, S_c and S_p factors of 0×0 field were obtained from the non-linear least square fit. And in our experiments, the measured and fitted output factors were within $\pm 0.2\%$ uncertainties for all field sizes.

The different amount of S_c factors for increasing field size showed larger than that of S_p factors for increasing field size.

DISCUSSIONS

According to Task Group 21 protocols¹¹⁾, the nominal accelerating potential of 23 MV photon beam from Mevatron KD 8067 was determined using the ratio of ionizations measured at 10 cm and 20 cm depth in water at a constant source-detector distance of 100 cm. the measured ionization ratio of TMR^{20}_{10} was obtained with 0.787 ± 0.002 which corresponds to a nominal accelerating potential of $18.5 \pm 0.5 \text{ MV}$ for this photon beam.

As recommended by the Task Group 21 protocol for 23 MV nominal X-rays, no scaling corrections for depth in polystyrene relative to depth in water were made.

In our study of nominal energy, however, the observed percentage depth dose for a $10 \times 10 \text{ cm}^2$ field with 100 cm SSD at a depth of 10 cm is 80.2%, and this percentage depth dose is set between at that of 21 MV and 25 MV X-rays in suggested on Ref. (5).

As the compared with results, for small field sizes, $10 \times 10 \text{ cm}^2$ or less, our experimental data are within 1% higher than suggested percentage depth dose of 21 MV X-rays, for large field sizes, but 4.5% higher than that of reference photon beam.

while the CL 1800¹⁾ has been showed the small

field sizes is within 1% less, and those of large field sizes are within 2.5% less than those of mevatron KD 8067 dual energy 23 MV photon beams.

In the beam flatness and symmetry, the high clinical quality of the beam is showed with average the $2.7 \pm 1.48\%$ of flatness and $1.13 \pm 0.79\%$ of symmetry at depth of 10 cm in water phantom. However the maximum off-axis dose of beam is 5.0% and 8.9% greater than the central axis dose at the depth of maximum dose of 20×20 and 30×30 cm² fields, respectively. this undesirable features would be induced the "hot spots" in the radiotherapy planning for large field irradiations.

The physical penumbra, separation between the 90% and the 20% isodose lines at d_{max} , had been estimated the width of 9.5 ± 0.5 mm in Fig. 3.

In our experiments, the percent surface doses increased from 3.2% to 25.3% without blocking tray as field sizes increased from 5×5 cm² to 25×25 cm², however it shows that the percent surface doses increased from 4.2% to 31.1% with blocking tray (thickness of 0.6 cm plastics) at the same field size and beam alignments. And estimated percentage of maximum depth dose in the buildup region showed the slope of increments is relatively smaller than that of lower photon energy^{1,3,6)}.

The average relative percent difference in the calculated and measured TMR's data showed within $0.3 \pm 0.5\%$ for all selected fields and depths. It means that this calculated TMR's data can be agreed to accept in clinical applications. the TMR's of zero field size were also derived from the three different methods and they has been showed average 2.3% uncertainty for 5 to 30 cm depths. Furthermore this TMR's of zero field size could be supplied to calculated the SMR's data. The smoothed and extended SMR's to large field by achieved fitting the SMR's of given field have been estimated within $3.3 \pm 2.0\%$ uncertainties at the large depths. These SMR's data are very helpful in calculating the dose distributions of large irregularly shaped fields.

In our experiments, the HVL of 23 MV photon beam from Mevatron KD 8067 dual energy showed with 24.5 g/cm². And this measured HVL with narrow beam geometry is a little higher than that of the 18 MV beam on a Varian Clinac 20 published by Johnson et al¹⁾.

SUMMARY

The characteristis of the 23 MV photon beams have been examined from a mevatron 8067 with respect to clinical parameters.

The nominal accelerating potential of this photon beams could be determined with 18.5 ± 0.5 MV.

In our experiment, the depth of 80% dose for a 10×10 cm² field at 100 cm SSD is 10.1 ± 0.1 cm, and percentage depth dose were set at between that of 21 and 25 MV photon beams on reference of BJR supplement NO 17.

The depth of maximum dose has been showed the variation from d_{max} of 2.8 cm for large field to that of 3.8 cm for small field, and it made some effective to calculate the TMR's and SMR's value.

The percentage surface dose showed 9.6% of d_{max} at 10×10 cm² field size without blocking tray in, and buildup region data were also obtained for a Mevatron KD 8067 dual energy linear accelerator with Capintec PS-033 parallel-plate ionization chamber.

REFERENCES

1. Johnson DA: Properties of the 18-MV photon beam from a dual energy linear accelerator. Med Phys 14:1071-1078, 1987
2. Paul JM, Richard F: Characteristics of mevatron 77 15-MV photon beam. Med phys 10:237-242, 1983
3. Velkkey DE, et al: Build-up region of megavoltage photon radiation sources. Med Phys 1:14-19, 1975
4. Arcovito G, Piermattei A: Dose measurements and claculations of small radiation fields for 9 MV X-rays. Med Phys 12:779-784, 1985
5. BRJ Supplement No. 17: Central axis depth dose data for use in radiotherapy. London, British Institute of Radiology 1983, pp 45-120
6. Tannous NBJ, et al: Buildup region and skin-dose measurements for the Therac 6 linear accelerator for radiation therapy. Med phys 8:378-381, 1981
7. Khan FM: A system of dosimetric claculations; The physics of radiation therapy. Baltimore/London, Williams & Wilkins 1984, pp 182-188
8. Keller B, et al: 10 MV photon beam characteristics; Central axis depth doses, Tissue-Maximum Ratios, Scatter-Maximum Ratios, Beam Flatness, Backscatter and Output Factors. Int J Oncol biol Phys 1: 69-75, 1975
9. Meli JA, Nath R: Choice of material for HVL measurements in megavoltage X-ray beams. Med Phys 12:108-110, 1985
10. Khan FM, Moore VC, et al: Depth dose and scatter analysis of 10 MV X-rays. Radiology 102:165-169, 1972
11. Task Group 21: A protocol for the determination of absorbed dose from high-energy photon and electron beams. Med Phys 10:741-771, 1983

= 국문초록 =

Mevatron KD 8067 선형가속기의 23 MV 광자선의 특성

계명대학교 의과대학 치료방사선과학교실

김옥배 · 최태진 · 김영훈

고 에너지 23 MV 광자선의 특성 중 임상적용에 중요한 심부선량 백분율, 조직-최대선량비 (TMR), 산란-최대선량비 (SMR), 표면선량 및 출력선량 보정계수등의 변수가 이온전리 (IC-10)함 및 평행 평판전리 (PS-033)함에 의해 측정 조사되었다.

명목상의 23 MV X-선에 대한 가속에너지는 18.5 ± 0.5 MV로 측정되었다.

Mevatron KD 8067의 23 MV X-선의 중심선속의 반가층이 기하학적인 좁은 선속으로 측정되었으며 반가층의 두께는 24.5 g/cm^2 이었다. 조직-최대선량비는 심부선량백분율표에서 구해졌으며, 실측치와 비교한 결과 각 조사면의 크기와 깊이에서 약간의 차이를 보였으나 평균 $0.7 \pm 0.5\%$ 의 오차를 나타내고 있어 계산에 의한 TMR 값과 잘 일치함을 보였다.

조사면 $0 \times 0 \text{ cm}^2$ 의 TMR 값은 zero 조사면의 유효감약계수에 의한 값과, 각 조사면의 조직-최대선량비로부터 비선형최소자승법에 의해 구해진 유효선흡수계수 및 반가층 측정에 의한 유효선흡수계수에 의한 값들로 비교되었으며, $\mu = 0.0283 \pm 0.0002 \text{ cm}^{-1}$ 을 보였고, 세 방법 모두 오차범위내에서 잘 일치됨을 보였다.

한편, 불규칙 조사면의 선량계산에 이용될 SMR은 조사면의 반경 50 cm까지 계산되어 대형 조사면에서도 선량을 산출이 이루어지도록 하였다.

Mevatron KD 8067의 23 MV X-선의 조직 표면선량은 SSD 100 cm, $10 \times 10 \text{ cm}^2$ 의 조사면에서 최대조직선량율의 9.6%, $25 \times 25 \text{ cm}^2$ 에서는 25.4%를 보였다.